Biochimica et Biophysica Acta 1787 (2009) 191–200

Contents lists available at ScienceDirect

Biochimica et Biophysica Acta

journal homepage: www.elsevier.com/locate/bbabio

Replacement of chlorophyll with di-vinyl chlorophyll in the antenna and reaction center complexes of the cyanobacterium *Synechocystis* sp. PCC 6803: Characterization of spectral and photochemical properties

Tatsuya Tomo [a,*], Seiji Akimoto [b,c], Hisashi Ito [d], Tohru Tsuchiya [a], Michitaka Fukuya [c], Ayumi Tanaka [d], Mamoru Mimuro [a]

[a] *Graduate School of Human and Environmental Studies, Kyoto University, Kyoto 606-8501, Japan*
[b] *Molecular Photoscience Research Center, Kobe University, Kobe 657-8501, Japan*
[c] *Graduate School of Science, Kobe University, Kobe 657-8501, Japan*
[d] *Institute of Low Temperature Sciences, Hokkaido University, Sapporo 060-0819, Japan*

ARTICLE INFO

Article history:
Received 19 November 2008
Received in revised form 26 December 2008
Accepted 30 December 2008
Available online 8 January 2009

Keywords:
Divinyl chlorophyll
Photosystem II
Delayed fluorescence
Cyanobacteria
Synechocystis sp. PCC 6803

ABSTRACT

Chlorophyll (Chl) *a* in a cyanobacterium *Synechocystis* sp. PCC 6803 was replaced with di-vinyl (DV)-Chl *a* by knock-out of the specific gene (*slr1923*), responsible for the reduction of a 8-vinyl group, and optical and photochemical properties of purified photosystem (PS) II complexes (DV-PS II) were investigated. We observed differences in the peak wavelengths of absorption and fluorescence spectra; however, replacement of Chl *a* with DV-Chl *a* had limited effects. On the contrary, photochemical reactions were highly sensitive to high-light treatments in the mutant. Specifically, DV-Chl *a* was rapidly bleached under high-light conditions, and we detected significant dissociation of complexes and degradation of D1 proteins (PsbA). By comparing the SDS-PAGE patterns observed in this study to those observed in spinach chloroplasts, this degradation is assigned to the acceptor-side photoinhibition. The delayed fluorescence in the nanosecond time region at 77 K was suppressed in DV-PS II, possibly increasing triplet formation of Chl molecules. Our findings provide insight into the evolutionary processes of cyanobacteria. The effects of pigment replacement on the optimization of reactions are discussed.

1. Introduction

Photosynthetic pigments, particularly chlorophylls (Chls), play crucial roles in the primary processes of photosynthesis of oxygenic photosynthetic organisms. Light absorption, resonance energy transfer, photochemical reaction, and quenching of excess light energy are typical examples of these processes. Nine Chl species [i.e., Chl *a*, Chl *b*, Chl *c*, Chl *d*, Chl *a*′ (13^2 epimer of Chl *a*), Chl *d*′ (13^2 epimer of Chl *d*), pheophytin *a* (Mg-free Chl *a*), di-vinyl (DV)-Chl *a* (Chl a_2), and DV-Chl *b* (Chl b_2)] are known to be confined in pigment–protein complexes [1,2]. With the exception of one taxonomic group (i.e., *Prochlorococcus* sp.), all other oxygenic photosynthetic organisms contain mono-vinyl (MV)-Chl *a*. Reduction of the 8-vinyl group on the pyrrole ring II of 3,8-DV-chlorophyllide (i.e., or 3,8-DV-protochlorophyllide) is a prerequisite for the synthesis of MV-Chl (i.e., Chl *a*, Chl *b*, Chl *c*, and Chl *d*), and a gene encoding the reducing enzyme is present in most oxygenic photosynthetic organisms [3]. Among these nine Chl species, Chl *a*, Chl *a*′, Chl *d* and DV-Chl *a* can serve as electron donors in photochemical reaction center (RC) complexes. In addition, several minor pigments species [i.e., Chl *a*′, Chl *d*′, and pheophytin (Pheo) *a*] constitute a frame for photochemical reactions in the RC. Furthermore, intermediates of Chl metabolism accumulate to detectable amounts under certain growth conditions.

The properties of pigments are modified via interactions with proteins. Energy levels and redox potentials in the ground and the excited states are directly affected by interactions with specific groups of amino acids and also with other Chls, and electric fields formed by protein moieties may confer additional effects. It is well known that hydrogen bonds affect the redox potential of primary electron donors in the RC of anoxygenic purple bacteria [4,5]. The stability of pigments in the complexes has not been well studied; however, stability is a primary requisite for function. Accommodation of pigments by protein moieties is accomplished via strict molecular interactions between pigments and amino acid residues.

In the course of acquisition of oxygenic photosynthesis in cyanobacteria, bacteriochlorophyll pigments are replaced with Chl pigments. This replacement occurs prior to the establishment of oxygenic photosynthesis, because the high potential (i.e., approximately

Abbreviations: Chl, chlorophyll; DF, delayed fluorescence; DV, di-vinyl; MV, mono-vinyl; Pheo, pheophytin; PS, photosystem; RC, reaction center; TDDFT, time-dependent density functional theory; TRFS, time-resolved fluorescence spectrum

* Corresponding author. Tel.: +81 75 753 9375; fax: +81 75 753 7909.
E-mail address: tomo@z05.mbox.media.kyoto-u.ac.jp (T. Tomo).

0005-2728/$ – see front matter © 2009 Elsevier B.V. All rights reserved.
doi:10.1016/j.bbabio.2008.12.014

+1.2 V) [6–8] is required for oxygenic photosynthesis. The oxidation potential of Chl *a* in CH_2Cl_2 is estimated to be 0.80 V [9–11], and additional potential is conferred via interactions with protein moieties. However, replacement of pigments always induces a partial loss in integrity of complexes. For switching of the biosynthesis pathway from bacteriochlorophyll *a* to Chl *a*, loss of several enzymes and acquisition of one enzyme are required. The second event in acquisition of oxygenic photosynthesis involves the modification of protein moieties, which stabilizes the replaced pigments in the complexes. Therefore, the replacement of pigments precedes stabilization with the protein moieties.

We have developed several experimental systems to reproduce the process of pigment replacement during oxygenic photosynthesis. For example, we introduced Chl *b* into a cyanobacterium (i.e., *Synechocystis* sp. PCC 6803, hereafter referred to as *Synechocystis*) [12], and introduced DV-Chl *a* into *Arabidopsis* [13]. The former example constitutes an experimental reproduction of the evolution from *Synechococcus* sp. to *Prochlorococcus* sp. [14,15]. These experiments successfully incorporated newly acquired pigments into pre-existing proteins, and the pigments retained their functions (e.g., light absorption and energy transfer in the antenna [12,15] or electron transfer in RC complexes [16]). However, introduction of DV-Chl *a* reduced tolerance to strong illumination [13,17,18], perhaps reflecting a partial loss in the integrity of the complexes. To identify the reasons for this loss in integrity, we isolated PS II complexes from DV-Chl *a* introduced into *Synechocystis*, and compared the properties of these complexes with those isolated from control cells. We observed acceptor-side photoinhibition in the mutant cells. Based on our observations, the integrity of pigments in pre-existing proteins and the evolution of cyanobacteria are discussed.

2. Materials and methods

2.1. Cyanobacterial culture

Synechocystis sp. PCC 6803 was engineered to express a 6×His-tag at the C-terminus of a 47 kDa chlorophyll-protein (i.e., CP47, PsbB) for use as a control. The control cells were constructed by site-directed mutagenesis [19]. A *slr1923* knock-out mutant of *Synechocystis*, which lacked a component of DV-protochlorophyllide reduction, was obtained on the basis of the above control cells using a method described previously [17]. Control and mutant cells were cultured under autotrophic conditions in BG 11 medium at 298 K, with illumination from an incandescent light (i.e., 20 μmol photons m^{-2} s^{-1}). Air was continuously supplied through a Myrex filter (Millipore, USA).

2.2. Pigment preparation

MV-Chl *a* and DV-Chl *a* were isolated from the thylakoid membranes of control and mutant cells of *Synechocystis*, respectively. All pigments were purified by HPLC with a JASCO GULLIVER series instrument (JASCO, Tokyo, Japan). Pigments were extracted with acetone, and the solvent was replaced with chloroform. Samples were injected into a Senshupak Silica-5301N column (300 mm×30 mm, Senshu Science., Tokyo, Japan) after filtration (0.2 μm). The mobile phase was hexane/2-propanol (100:2) with a flow rate of 5.0 ml/min. Pigments were detected by a photodiode-array detector (JASCO, MD-915, Tokyo, Japan). The absorption spectra of Chls were measured using a Cary 500 spectrophotometer.

2.3. Isolation of PS II complexes

We isolated PS II complexes from control and mutant cells using a His-tag introduced at the C-terminus of CP47. Thylakoid membranes were isolated via mechanical disruption and differential centrifugation. The resulting PS II was solubilized using a detergent (i.e., dodecyl-β-D-maltoside, 0.8%) for 20 min at 277 K in the dark, and purified by Ni^{2+}-affinity column chromatography [20].

2.4. Assay of oxygen-evolving activity

Oxygen-evolving activity was measured using a Clark-type oxygen electrode (Rank Brothers, England) at 298 K with 6 mM potassium ferricyanide as an electron acceptor. The measurements were carried out in a buffer solution (50 mM MES, pH 6.0) containing 1.0 M sucrose, 20 mM $CaCl_2$, and 10 mM NaCl.

2.5. Photochemical reactions

Pigment photobleaching was monitored using a Hitachi photodiode-array spectrophotometer (Hitachi 0080D, Japan). For actinic light, blue light was provided from a slide projector with heat- and UV-absorbing filters (HA-50, Toshiba, Japan) and spectral differences in the red region were monitored. The intensity of actinic light was 1000 μmol photons m^{-2} s^{-1}. The Chl contents were spectroscopically determined using a combination of 80% acetone extraction with the reported extinction coefficient by Porra et al. [21].

2.6. Degradation of D1 proteins

Degradation of D1 proteins was monitored via gel-electrophoresis of component proteins. After illumination of red light over a certain time period (i.e., from 0 min to 60 min, 2500 μmol photons m^{-2} s^{-1}), aliquots were sampled and SDS-PAGE patterns were compared. The D1 protein and its degradation products were identified using an anti-D1 antibody (AgriSera, Sweden) raised against the C- and N-termini of the D1 protein [22]. An antibody raised against the 43 kDa chlorophyll-protein (i.e., CP43, PsbC) (AgriSera, Sweden) was also used for protein identification.

2.7. Spectroscopy

Absorption spectra were measured using a Cary 500 spectrophotometer; for low-temperature spectra, a cryostat for liquid nitrogen temperatures (OptistatDN, Oxford Inst. Oxford, UK) was used in conjunction with a controller (Oxford ITC-601PT). Fluorescence spectra at 77 K were measured with a Hitachi 850 spectrofluorometer (Hitachi, Japan) with a custom-made Dewar bottle [23,24]. To assess low-temperature fluorescence spectrum, polyethylene glycol (i.e., PEG, average molecular weight 3350, final concentration 15% (w/v), Sigma-Aldrich) was added to obtain a homogeneous glass. The spectral sensitivity of the fluorometer was corrected using a sub-standard lamp with a known radiation profile. Time-resolved fluorescence spectrum and fluorescence decay curves were measured using time-correlated single-photon counting methods [22], with an excitation wavelength of 425 nm (i.e., the second harmonic of the 850-nm oscillation). Fluorescence lifetime was estimated via the convolution calculation [25].

2.8. Calculation of geometry optimization and energy levels for MV- and DV-Chl a

All calculations were performed using GAUSSIAN 03 [26]. The initial coordinates of atoms in the model Chl compound were obtained from the crystal structure of MV-chlorophyllide *a* [27]. Geometry optimization of MV- and DV-Chl *a* was performed using the DFT method, with Becke's three-parameter hybrid functional set [28] combined with the Lee–Yang–Parr correlation functional set (B3LYP) [29] and the 6–31G(d) basis set. For these molecules, the energy levels of singlet and triplet states were estimated via the

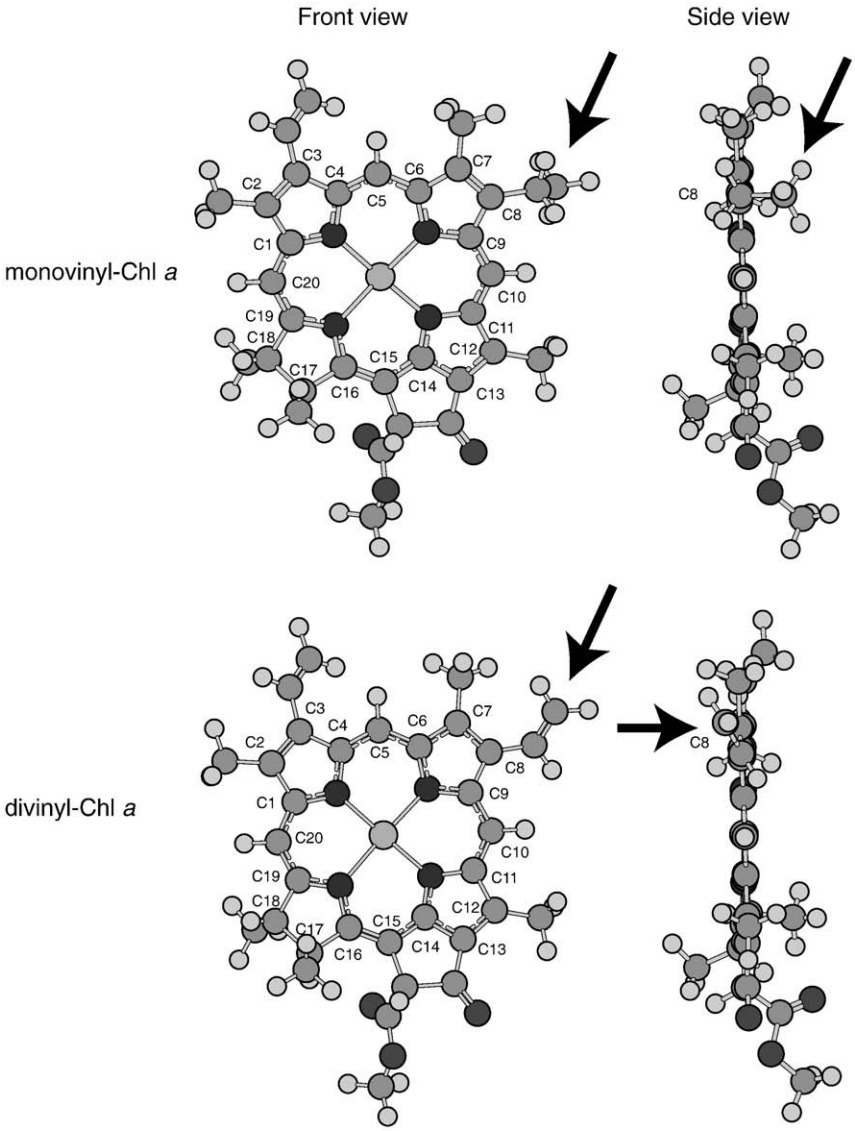

Fig. 1. Optimized structures of MV-Chl *a* and DV-Chl *a*. Structures were estimated via DFT calculations at the level of B3LYP/6-31G(d). Arrows indicate the C8 side-chain of Chls.

time-dependent density functional theory (TDDFT), using the same functional set and the 6–31+G(d) basis set.

3. Results

3.1. Optimized structures of MV- and DV-Chl a in vacuo at 0 K

The optimized structures of MV- and DV-Chl *a* without the phytol chains are shown in Fig. 1 as front and side views. The arrows indicated the C8 side-chain. In MV-Chl *a*, the C8-ethyl side-chain was perpendicular to the ring plane. However, the direction of the C8-vinyl side-chain was almost parallel to the ring plane in DV-Chl *a*. The structures of Chls in a protein matrix would not necessarily correspond to the calculated structures *in vacuo* at 0 K. A slight distortion of the ring and side chains of Chls is expected in proteins judging from crystal structures. However, these calculated structures were the origin for consideration in this study.

3.2. Absorption spectra

Fig. 2 shows the absorption spectra of DV- and MV-Chl *a* in acetone. The absorption maximum of the Qy band in DV- and MV-Chl

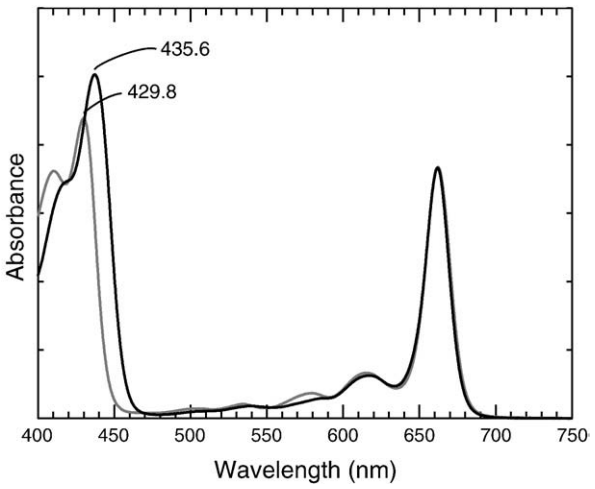

Fig. 2. Absorption spectra of MV-Chl *a* and DV-Chl *a* in acetone. Spectra were measured at room temperature (approximately 298 K). Black and gray curves represent DV-Chl *a* and MV-Chl *a*, respectively. Chl concentrations were 5 μg ml^{-1}.

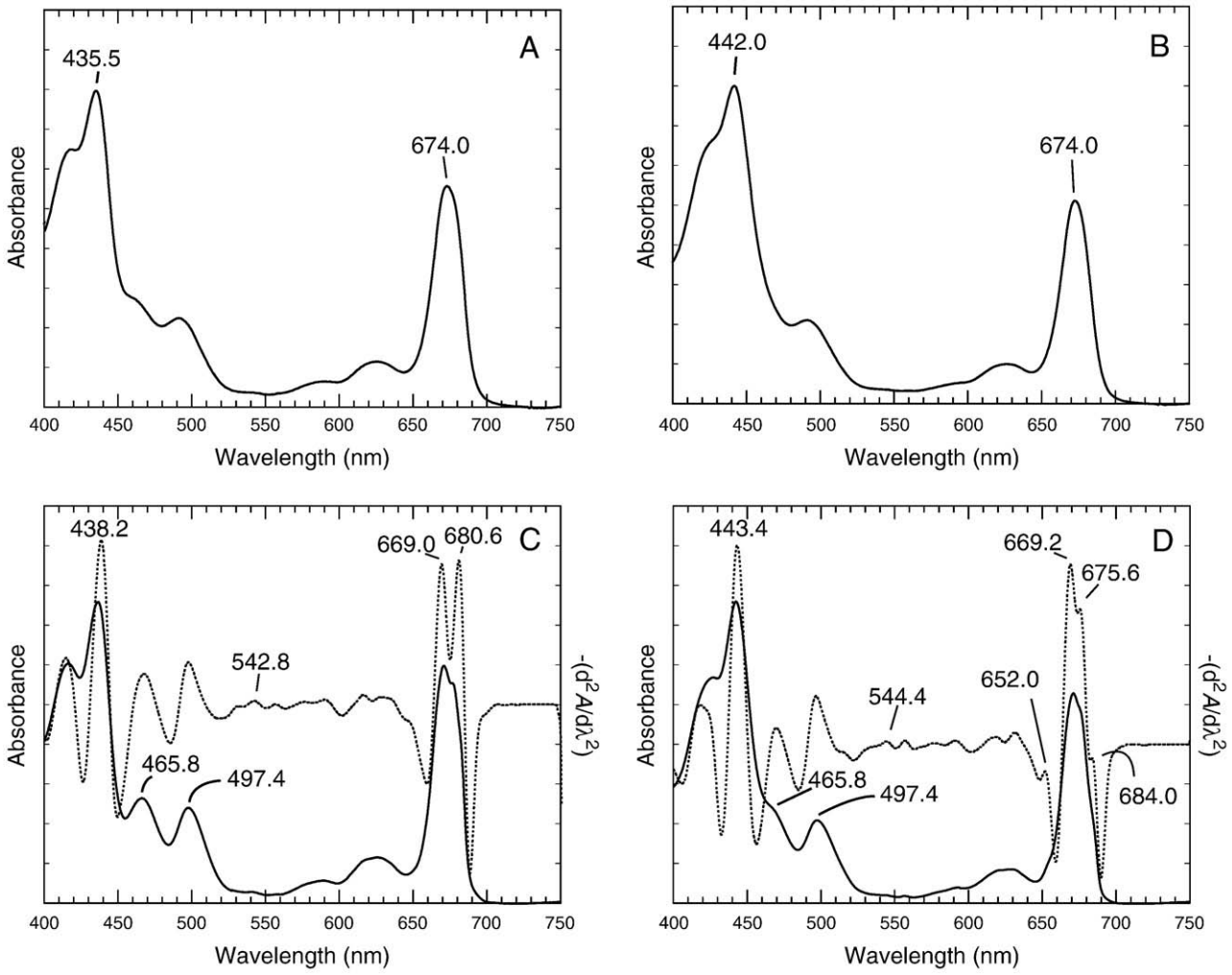

Fig. 3. Absorption spectra of PS II complexes with MV-Chl *a* and DV-Chl *a*. (A) and (C), PS II complexes with MV-Chl *a*. (B) and (D), PS II complexes with DV-Chl *a*. Spectra were measured at room temperature (i.e., A and B) and at 80 K (i.e., C and D). In (C) and (D), the second derivative spectra were shown after inversion. Chl concentrations were 5 μg ml^{-1}.

a were located at 661.8 nm and 662.2 nm, respectively. The peak maximum was slightly blue shifted in DV-Chl *a*. However, the Soret bands of DV-Chl *a* was significantly shifted by 5.8 nm to the red, compared with MV-Chl *a* (Fig. 2). The vibrational structures of the Qy and/or Qx bands were slightly different. These spectra were consistent with the spectra of a previous report [30].

The absorption spectra of isolated PS II complexes with MV-Chl *a* (MV-PS II) and DV-Chl *a* (DV-PS II) are shown in Fig. 3. The Chl content

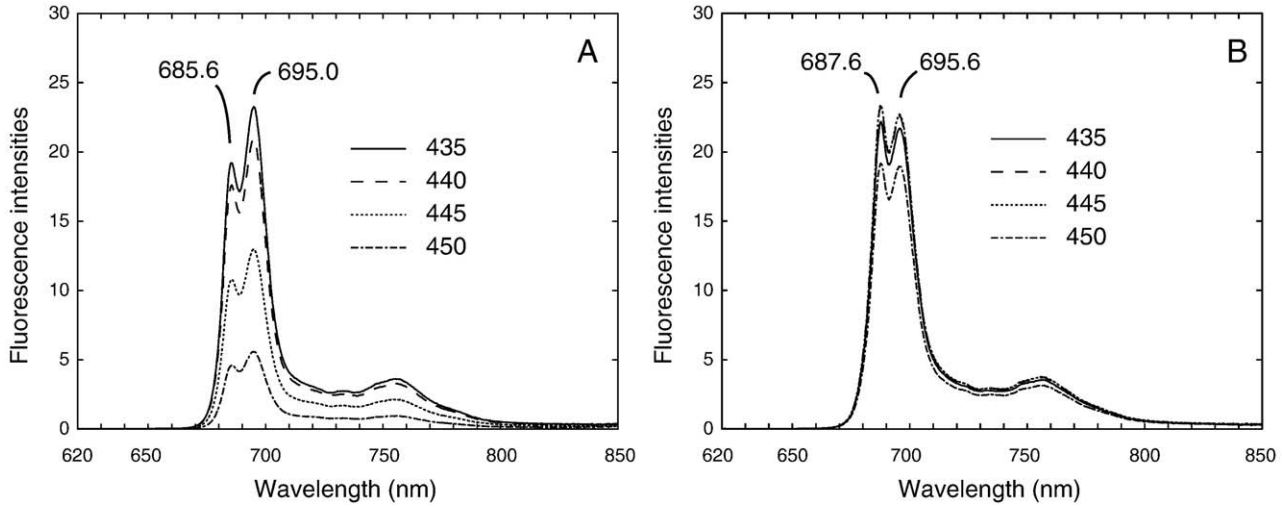

Fig. 4. Fluorescence spectra of PS II complexes with MV-Chl *a* and DV-Chl *a*. (A) PS II complex with MV-Chl *a*. (B) PS II complex with DV-Chl *a*. Spectra were measured at 77 K. Excitation wavelengths were selected to excite the Soret band of Chl *a*, and to monitor changes resulting from different wavelengths. Chl concentrations were 2 μg ml^{-1}.

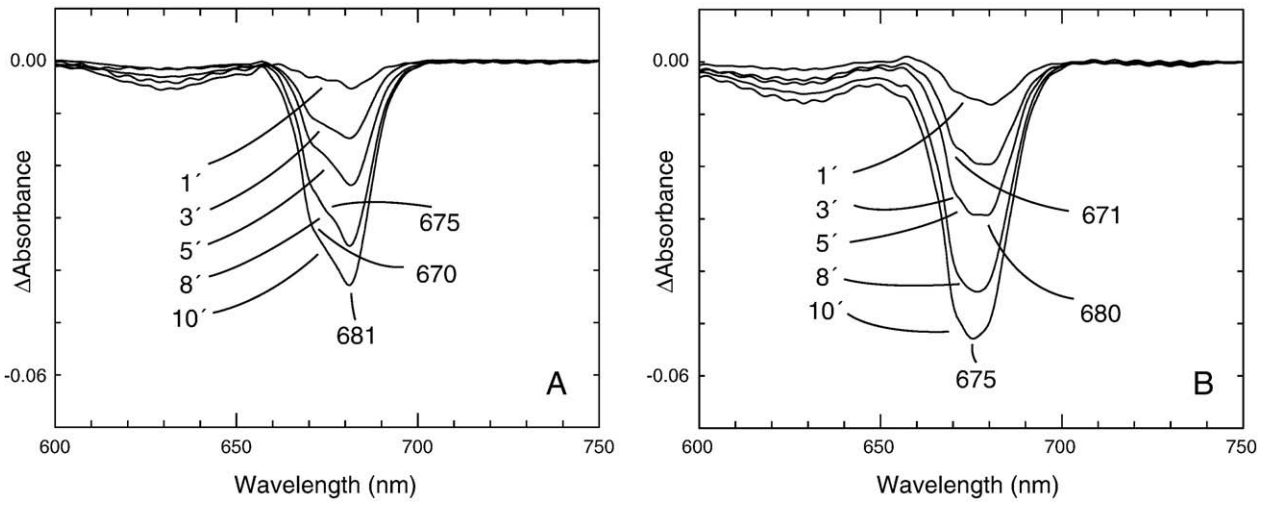

Fig. 5. Bleaching of Chl *a* in response to strong light illumination. (A) PS II complex with MV-Chl *a*. (B) PS II complex with DV-Chl *a*. Absorption changes in the red region were monitored in response to blue light illumination. Chl concentrations were 3.3 μg ml^{-1}. Absorption spectra were assessed after 1, 3, 5, 8, and 10 min of illumination with an intensity of 1000 μmol photons m^{-2} s^{-1}.

of PS II was estimated to be approximately 40 per two Pheo *a* in both samples. At room temperature, the Qy bands of the two samples were located at identical wavelengths (i.e., 674.0 nm) (Fig. 3A and B). However, the Soret bands of PS II complexes isolated from DV-PS II (Fig. 3B) shifted by 6.5 nm to the red, compared with those of PS II complexes isolated from MV-PS II (Fig. 3A). This tendency was the same as observed for isolated pigments (Fig. 2). At 80 K, the Qy band of DV-PS II (Fig. 3D) differed from that of MV-PS II (Fig. 3C). Apparent peaks were identified at 671.0 nm and 671.2 nm for MV-PS II and DV-PS II, respectively. The bandwidth of DV-PS II was somewhat narrower than that of MV-PS II, resulting from smaller contributions by long-wavelength components. In the second derivative spectrum, two major bands were resolved at 669.0 and 680.6 nm for MV-PS II; however, one component (i.e., located at approximately 676 nm) was not resolved. Three components were resolved at 669.2, 675.6 and 684.0 nm for DV-PS II. An additional component was discernible at approximately 652.0 nm for DV-PS II; however, corresponding components were not present in MV-PS II. These results indicate that the spectral components were similar to each other, but that their relative contents changed depending on the samples. The red shift of the Soret band in DV-PS II was clearly observed, and there were no indications of red-Chls in these preparations.

Bands corresponding to Pheo *a* were resolved on the second derivative spectra at 542.8 nm and 544.4 nm for MV-PS II and DV-PS II, respectively. Two peaks, corresponding to the carotenoid band, were clearly observed on the 80 K spectra. These peaks were located at 465.8 and 497.4 nm in both preparations. The spectral forms of the two carotenoid bands were very similar.

3.3. Fluorescence spectra

The fluorescence emission spectra were assessed via excitation of the Soret band at 77 K (Fig. 4). Variation of the excitation wavelengths had minor effects on the spectra. Two bands, at 685.6 nm and 695.0 nm, were observed for MV-PS II (Fig. 4A) and corresponded to typical PS II fluorescence components [31,32]. The

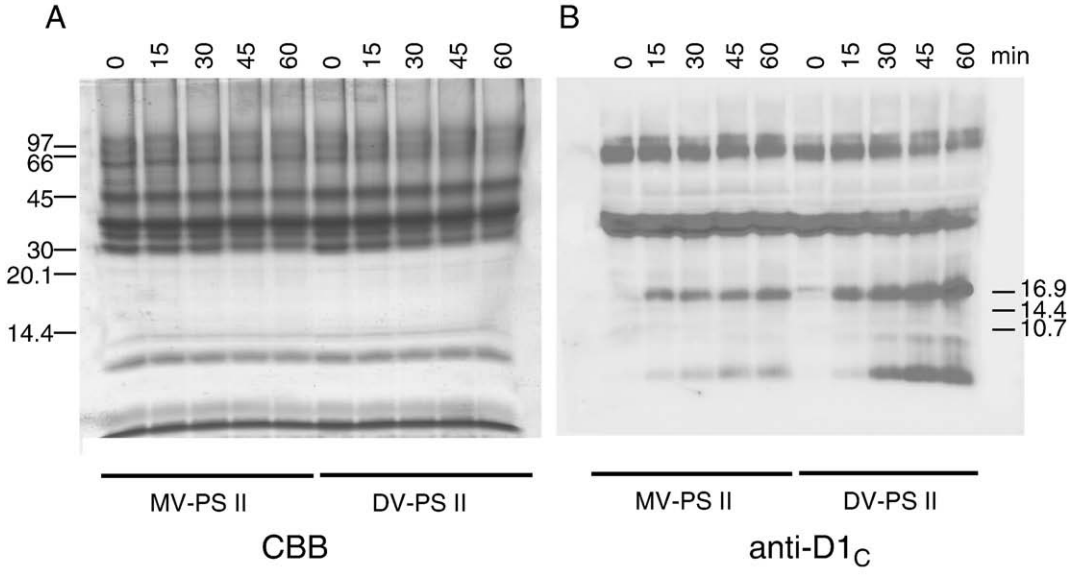

Fig. 6. Degradation of PS II polypeptides in response to strong light illumination. (A) SDS-PAGE profiles. (B) Detection of subunits by Western blotting with an anti-D1 C-terminal domain antibody. PS II complexes were illuminated at 298 K for 0, 15, 30, 45, and 60 min at 2500 μmol photons m^{-2} s^{-1}. Chl concentrations were 0.2 mg ml^{-1}.

relative intensity of the 695.0-nm component was always higher than that of the 685.6-nm component. Similar components were also detected for DV-PS II (Fig. 4B); however, the short-wavelength form shifted to the red region by 2 nm with the long-wavelength form keeping almost the same wavelength. The relative intensity of the short-wavelength form was higher than that of the long-wavelength form. The 756-nm emission band, the vibration band of Chl emission, was almost the same intensity when data were normalized at 695 nm. These findings indicate that changes in Chl species modulate a specific fluorescence component. As this component does not originate from the RC, a specific antenna (i.e., probably CP43) may contribute to this change. A shift in the short-wavelength component was also observed in the fluorescence spectra of intact cells and of the thylakoid membranes with DV-Chl *a* (data not shown).

3.4. Oxygen-evolving activity

The oxygen-evolving activities of the two preparations were nearly equal under a saturating light intensity. The activities of the isolated PS II complexes was 2200 μmol O_2 (mg Chl)$^{-1}$ h^{-1} and 2100 μmol O_2 (mg Chl)$^{-1}$ h^{-1} for MV- and DV-PS II, respectively.

3.5. Photochemical reactions

We previously reported that DV-Chl cells exhibited a rapid bleaching response to high-light, although the reasons for this phenomenon remain unclear. This effect is also observed in *Arabidopsis* [13] and *Synechocystis* [17]. Therefore, we investigated this phenomenon by following pigment bleaching and via the degradation of polypeptides.

3.5.1. Pigment bleaching

Light-induced bleaching of the Qy band of Chls is illustrated in Fig. 5. Upon illumination with blue light, MV-PS II was maximally bleached at 681 nm, followed by two other peaks at 670 and 675 nm (Fig. 5A). This pattern was essentially identical to that observed for spinach PS II RC [33,34]. The bleaching pattern of DV-PS II differed (Fig. 5B), as a main band was observed at 675 nm, followed by two additional bands at 671 and 680 nm. The bandwidth of the bleached band was wider in DV-PS II than in MV-PS II. We estimated a bleaching rate using the molecular coefficients of MV-Chl *a* and DV-Chl *a* [30]. Since the coefficient for DV-Chl *a* was smaller than that of MV-Chl *a*, the magnitude of bleach gave rise to a faster bleaching in DV-PS II by 30 to 60% within 10 min photo irradiation. These data indicate that the Chl species responsible for bleaching were identical in both samples, but that their relative reaction rates were greatly different.

3.5.2. Degradation of the D1 protein

We examined the degradation of the D1 polypeptide via SDS-PAGE and Western blot analysis (Fig. 6). Upon blue light illumination with 2500 μmol photons m^{-2} s^{-1}, the overall polypeptide patterns of the two samples were very similar (Fig. 6A, CBB stain). In contrast, the degradation of the D1 proteins continuously proceeded. The products of the degraded polypeptides were identified using antibodies raised against the C-terminal and N-terminal domains of the D1 protein. The anti-D1 C-terminal domain antibody detected two bands with molecular weights of 16 kDa and 8 kDa. The amounts of the products increased with time, and the reaction proceeded much faster in DV-PS II than in MV-PS II (Fig. 6B). The magnitude of breakdown products of D1 protein gave rise to a faster degradation in DV-PS II by 30 to 70%. The anti-D1 N-terminus antibody detected a 23 kDa molecular weight band in DV-PS II that increased with time (data not shown).

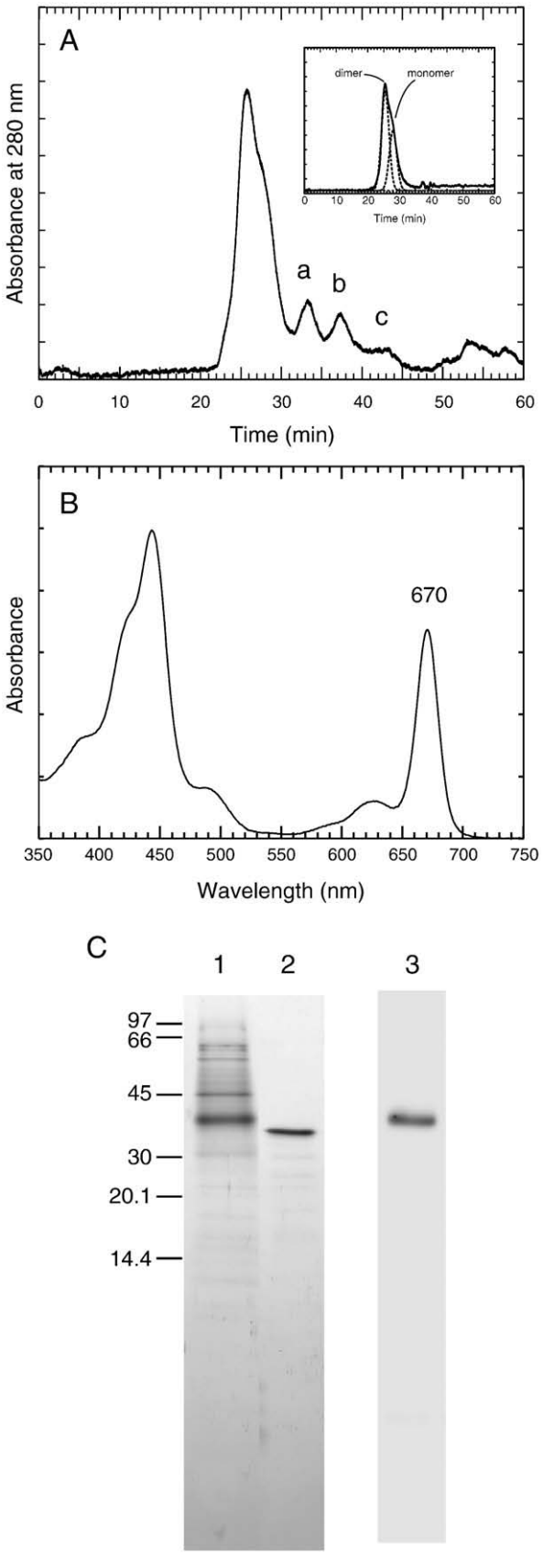

Fig. 7. Changes in the association state of the DV-PS II induced by strong light illumination. (A) Elution profile resulting from size-exclusion column chromatography of DV-PS II in response to high-light treatment. Inset indicates results before high-light treatment. (B) Absorption spectrum of sub-fraction a, assessed via size-exclusion chromatography. (C) SDS-PAGE profiles stained with CBB (i.e., lanes 1, 2) and Western blot analysis (i.e., lane 3) of sub-fractions from size-exclusion chromatography. Lane 1, sub-fraction a; lane 2, sub-fraction c; and lane 3, sub-fraction a reacted with anti-PsbC antibody.

Based on previous studies of higher plant PS II, the degradation pattern observed in this study was similar to the so-called acceptor-side photoinhibition [35–37]. It is well known that acceptor-side photoinhibition is induced via formation of a singlet oxygen ($^1O_2$), in response to the triplet state of a special pair (P_{D1} and P_{D2}) or an accessory Chl molecule (Chl_{D1}) [37]. Replacement with DV-Chl *a* is more likely to induce formation of the triplet state of Chl *a* in PS II complexes than in control cells.

3.6. Changes in the association state of the complexes

After photoinhibition, we detected changes in the coupled association states (Fig. 7A). Prior to illumination with a strong light (Fig. 7A, inset), most DV-PS II complexes were present in dimeric forms, as shown using size-exclusion chromatography (Superdex 200, GE Healthcare, USA). After illumination with a strong blue light (i.e. 1500 μmol photons m^{-2} s^{-1}, for 30 min), the number of monomers increased, and new peaks were detected in the low molecular weight region (Fig. 7A). One of those peaks (i.e., peak a in Fig. 7A) was determined to be CP43, based on the absorption spectrum (Fig. 7B), the SDS-PAGE profile (Fig. 7C, lane 1) and Western blotting analysis (Fig. 7C, lane 3). Peak c contained the PsbO protein, a peripheral protein involved in water oxidation, as indicated by the molecular weight via SDS-PAGE (Fig. 7C, lane 2). The origin of peak b was not identified. Light illumination induced partial dissociation of the complexes, which may account for the degradation of the complexes and photoinhibition.

3.7. Fluorescence decay (i.e., delayed fluorescence)

To monitor the photochemical reactions, we assessed the fluorescence decay curves in the nanosecond time region at 77 K, at wavelengths where delayed fluorescence (DF) was expected [20]. The gray line in Fig. 8 illustrates a typical decay curve at 685 nm, including DF in MV-PS II. The amplitude of DF corresponded to 0.2% of the total fluorescence, and the DF lifetime was 23.0 ns. In DV-PS II isolated from *Synechocystis*, DF was detected as a faint decay component of the 685-nm decay; its relative amplitude was 0.1%, with a lifetime of 27.1 ns (Fig. 8, black line). We were unable to detect DF on cells or thylakoid membranes containing DV-Chl *a* in *Synechocystis* (data not shown);

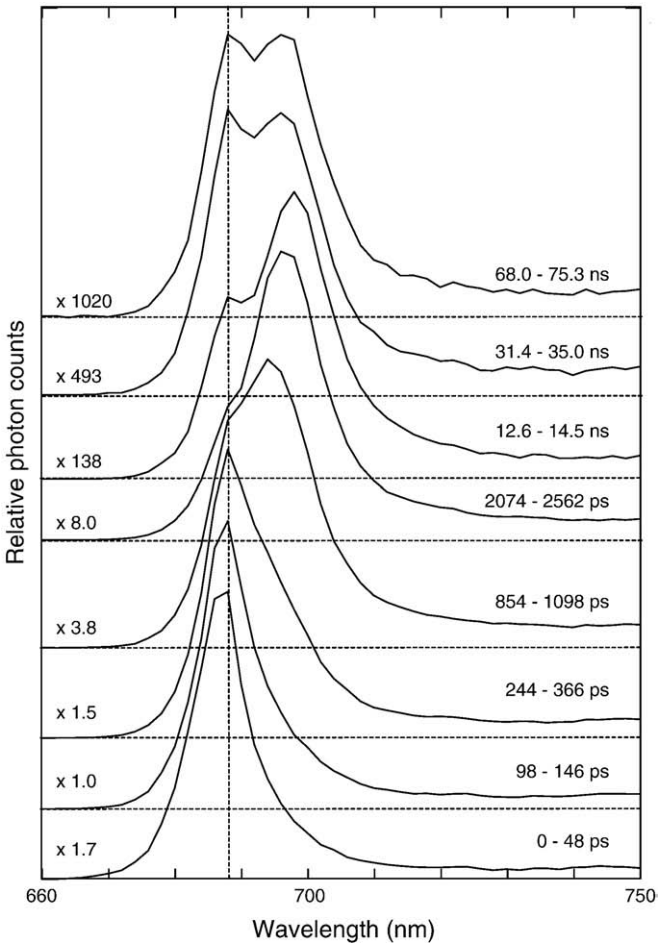

Fig. 9. TRFS of *Synechocystis* of PS II complexes with MV-Chl *a* and DV-Chl *a*. TRFS was measured at 77 K. The excitation wavelength was 425 nm, with a pulse width of 80 fs. The data acquisition interval was approximately 2 nm, and the acquisition time was 24.4 ps/channel. The half bandwidth of the monochrometer was 3 nm. Fluorescence intensities were normalized to the maxima of individual spectra. Numbers on the left side of the spectra indicate the magnification factor used to normalize data to the maximum photon counts. A vertical line indicates a location of the peak at 688 nm. Chl concentrations were 2 μg ml^{-1}.

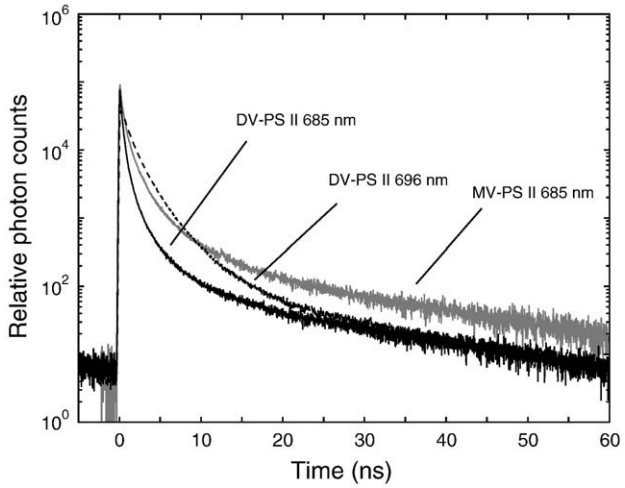

Fig. 8. Fluorescence decay curves at 77 K for *Synechocystis* PS II complexes with MV-Chl *a* and DV-Chl *a*. Fluorescence decay curves were monitored for the typical bands of Chl *a* fluorescence in the respective PS II complexes [i.e., 685 nm (solid line) and 696 nm (dashed line) in DV-PSII, and 685 nm (gray line) in MV-PS II]. The excitation wavelength was 425 nm. Chl concentrations were 2 μg ml^{-1}.

nor were we able to detect DF in *Arabidopsis* thylakoids containing DV-Chl *a* [16]. Since DF is observed as one of decay components in the total fluorescence, a relative amplitude of DF is higher when the antenna size is smaller; a high amplitude of DF (0.8%) was observed in the PS II reaction center complexes isolated from spinach [38] that contains a very small number of pigments, and this was a direct proof for the above relationship. However, even in the same antenna size in MV- and DV-PS II of *Synechocystis*, a difference in the DF amplitude was observed, reflecting an intrinsic property of the two preparations. A low amplitude of DF was assigned to one of major differences in the DV-PS II preparations [16], as our results were consistent with previous studies of *Arabidopsis* thylakoids containing DV-Chl *a*. At 696 nm, a long-lived component was also observed, corresponding to a long-wavelength tail of the 685-nm component [20]. These results clearly indicated that replacement of MV-Chl *a* with DV-Chl *a* suppressed DF, even if DF did not completely disappear. This was considered a unique property of DV-PS II.

3.8. Time-resolved fluorescence spectrum

The time-resolved fluorescence spectrum (TRFS) of DV-PS II is shown in Fig. 9. We observed two fluorescence components with peaks of 687 and 696 nm, corresponding to the steady-state spectrum

(Fig. 4B). An additional band, whose maximum was located at a wavelength slightly shorter than 687 nm, was observed in the initial time range; however, the origin of this band was not determined. The 687-nm band predominantly appeared after excitation at 425 nm, and exhibited a narrow bandwidth. After a certain period after excitation (i.e., approximately 200 ps), the second component appeared at 696 nm. The relative intensity of this component increased rapidly and remained dominant until 35 ns. However, the relative intensity of the first component (i.e., the 687-nm component) increased again after this time. These changes indicate that the major decay components have distinct lifetimes (i.e., 437 ps and 1.54 ns for the 686 nm band, and 1.96 ns and 3.65 ns for the 696 nm band). The increased relative intensity at 686 nm during the later time range indicated that DF was present at this wavelength, even though the yield of DF was negligible by decay analysis but was detectable by TRFS analysis.

3.9. Energy differences in the triplet and singlet states of Chl

The energy levels of S_1 state *in vacuo* and at 0 K were determined to be 2.1129 eV and 2.1078 eV for MV-Chl *a* and DV-Chl *a*, respectively. The energy level of the S_1 state of MV-Chl *a* was almost identical to that reported by Vokáčová and Burda [39]. The energy levels of the T_1 state were estimated to be 1.3330 eV and 1.3464 eV in MV-Chl *a* and DV-Chl *a*, respectively. The energy gap between the singlet and triplet states in DV-Chl *a* was smaller by 18.5 meV than that in MV-Chl *a*. This might be one reason for differences in the reaction processes in the PS II complexes.

4. Discussion

4.1. Accommodation of pigments in mutant cells

The function of pigments is largely determined by the electronic states; these are modified by interactions with protein moieties. Replacement of pigments may alter interactions with pre-existing proteins. The directions of the ethyl and vinyl groups of the C8 side-chains differed in MV- and DV-Chl *a* (Fig. 1). Therefore, steric hindrance was expected to occur in DV-PS II. Six Chl *a* and two Pheo *a* molecules were identified in the D1 and D2 proteins of *Synechocystis* [40]. Steric hindrance between P_{D1} and Chl_{D1} (Fig. 10), and P_{D2} and Chl_{D2} (data not shown), was predicted from the crystal structure [41]. The distance between the plane of ring V at P_{D1} and the hydrogen atom of the C8 vinyl group at Chl_{D1} was less than 1.1 Å, as determined via simulation analysis (Fig. 10). Steric hindrance may cause changes in the distance or orientation between pigments, which should then alter the reaction processes or the charge distribution between the P_{D1} and Chl_{D1} molecules. When DV-Chl *a* was introduced into *Arabidopsis* thylakoids [16] and into the cell and thylakoid membranes of *Synechocystis* (data not shown), we did not observe DF in the 10-ns time region at 77 K. Similar results were obtained in the present study (i.e., a lower amplitude was observed for the DF from isolated DV-PS II) (Fig. 8). The DF observed in the 10-ns time region at 77 K originated from the recombination between the special pair or the Chl_{D1} and Pheo *a* in PS II [20]. Therefore, the reduced amplitude of DF in the DV mutant may have resulted from a change in the charge distribution, accompanied by steric hindrance. However, several amino acids are located within close vicinity (i.e., less than 5 Å) of the C8 side-chain of DV-Chl *a* in the P_{D1}, P_{D2}, active Pheo *a* and inactive Pheo *a* molecules of the PS II RC complexes. Therefore, additional effects on steric hindrance cannot be excluded. Accommodation of new pigments in the pre-existing proteins appeared to have been altered.

4.2. Photoinhibition

Previous studies have shown that the turnover rate of the D1 protein in PS II RC is higher than that of any other proteins in the thylakoid membrane under illumination *in vivo*. The mechanisms of D1 protein degradation have been intensively studied *in vitro*, particularly using isolated PS II preparations [37,42]. The FtsH protease is a candidate enzyme involved in D1 digestion. However, the FtsH protease digests the 22 kDa fragment [43,44], and the 16–18 kDa fragments do not appear to be digested by this protease. Mizusawa et al. reported that the initial damage to the D1 protein under illumination *in vitro* was similar to that observed *in vivo*; however, further degradation of fragments and adducts occurred in the *in vivo* systems [45]. Taken together, these findings suggest that, once damaged, the D1 protein is thoroughly degraded by several proteases that digest abnormal proteins. Therefore, an analysis of the initial degradation products of the isolated PS II complex is warranted for studies of photoinhibition. The degradation profile of the D1 protein revealed that acceptor-side photoinhibition was enhanced in DV-PS II (Fig. 6B). In general, singlet oxygen molecules are responsible for acceptor-side photoinhibition [37]. The formation of singlet oxygen molecules is initiated by the triplet state of Chl. This state is induced by charge recombinations between the electron donor (i.e., P_{D1} or Chl_{D1}) and the primary electron acceptor (i.e., Pheo *a*), followed by intersystem crossing. In the triplet state, a spin exchange reaction between the triplet state of Chl and the triplet state of oxygen (i.e., the ground state of oxygen) gives rise to singlet oxygen molecules. In PS II, it is well known that Chl_{D1} accumulates a triplet state [46,47]. Thus,

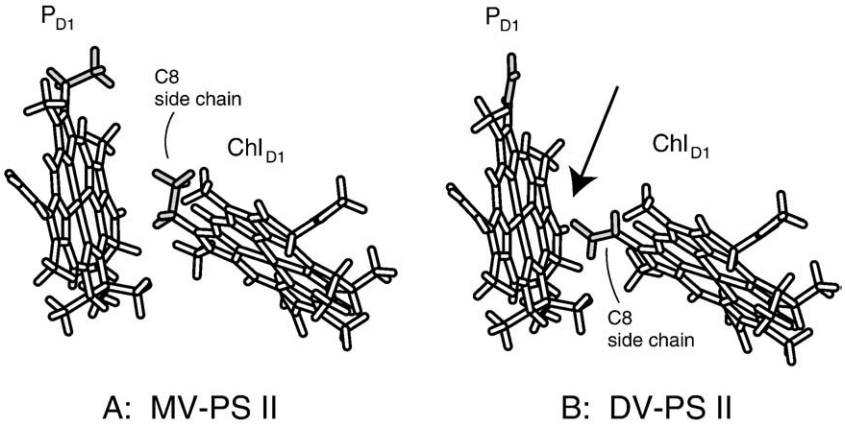

Fig. 10. Simulation of the Chl_{D1} and P_{D1} structures in PS II complex with MV- and DV-Chl *a*. Locations of Chl_{D1} and P_{D1} in the most stable form of the PS II reaction center were estimated based on the crystal structure of cyanobacterial photosystem II (PDB code: 2AXT; 3.0 Å resolution). (A) PS II complex with MV-Chl *a*. (B) PS II complex with DV-Chl *a*. Gray colours represent C8-side chain of each Chls. The arrows indicated the expected steric hindrance site at PS II complex with DV-Chl *a*.

triplet formation and DF compete after charge recombination. We did not estimate the yield of triplets formed in DV-PS II; however, the relatively low yield of DF in DV-PS II suggests a higher yield of triplet formation, which would lead to the formation of singlet oxygen molecules. Our TDDFT analysis also indicated that the energy difference between S_1 and T_1 in DV-Chl *a* was 18.5 meV smaller than that in MV-Chl *a* (with an approximately 780 meV total difference). The calculated energy level of DV-Chl *a* was red-shifted in comparison with the experimental results. If these values can directly be applied to DV-PS II, the conversion from S_1 to T_1 may be favorable in DV-PS II.

4.3. Rapid bleaching and dissociation of PS II

The rate of Chl bleaching was faster in DV-PS II than in MV-PS II by 30 to 60%. In response to high-light treatment, *slr1923* mutant cells were completely bleached after 1 day (i.e., within a few hours of the high-light treatment), while control cells appeared slightly yellow in color [17]. As the turnover of the D1 protein is determined by differences in synthesis and degradation, the rate of D1 degradation seems much higher than the *de novo* synthesis rate. The rapid bleaching process is a typical phenotype of the DV mutant. This phenomenon cannot be explained only by accepter-side photoinhibition. Components of the PS II subunit (i.e., CP43 and PsbO) were dissociated by the high-light treatment (Fig. 6). The CP43 is a candidate ligand of the Mn-cluster, and PsbO is an indispensable subunit involved in the stabilization of the Mn-cluster [48,49]. Therefore, donor-side inactivation is also expected to occur under high-light conditions, perhaps contributing to the rapid bleaching observed in DV-PS II.

4.4. Evolution of cyanobacteria

Prochlorococcus species lack DV-protochlorophyllide reductase; therefore, all Chl obtained from *Prochlorococcus* were of the DV type. *Prochlorococcus* can be classified into two main ecotypes: a high-light adapted ecotype and a low-light adapted ecotype. Phylogenetic analyses (i.e., based on 16S rDNA sequences) suggest that high-light adapted *Prochlorococcus* species branched out after evolution of the low light-adapted ecotype [50]. The overall identity of the PsbA sequence has been well conserved (i.e., 83.4–86.4%) between *Synechocystis* and *Prochlorococcus* (i.e., *Prochlorococcus marinus* MED4, *P. marinus* MIT9313, *P. marinus* NATL2A, and *P. marinus* SS120) (Cyanobase, Kazusa). The amino acids located near the C8 side-chain of DV-Chl *a* in PsbA have also been conserved between *Synechocystis* and *Prochlorococcus*. Therefore, similar steric hindrance occurs in *Prochlorococcus* and in the DV mutant of *Synechocystis*. The steric hindrance at Chl_{D1} and P_{D1} of PS II is one of the reasons why low-light adapted *Prochlorococcus* cannot survive under high-light conditions. High-light adapted *Prochlorococcus* seem to have acquired additional phototolerant mechanisms, as determined via genomic analyses [50]. However, the reasons for high-light adaptation have not yet been determined.

Changes in pigment species occurred a few times during the evolution of cyanobacteria (i.e., acquisition of Chl *b* in *Prochloron* and *Prochlorothrix*, of DV-Chl *a* and DV-Chl *b* in *Prochlorococcus*, and of Chl *d* in *Acaryochloris marina*). With the exception of Chl *d* biosynthesis, the enzymes responsible for such changes have been elucidated and changes in one gene are known to induce changes in pigment species. However, our findings illustrate that optimization of amino acid sequences and the three-dimensional structures is the second step required for full optimization. This is an important concept required for the full understanding of the evolutionary pathways of cyanobacteria. In terms of species differentiation or survival of a new-born species, a small difference in the survival ratio of specific organisms will induce difference in the succession of those after a certain generations. Photo-induced damage to photosynthetic organisms may be a critical factor for evolution of organisms.

In summary, we characterized the PS II complexes of DV-Chl *a*-expressing *Synechocystis*. Based on the optical properties and photochemical reactions observed in our study, we conclude that the rapid bleaching of Chl *a* in the DV mutant occurs in response to impaired PS II. These reaction processes are not yet fully understood. The bleaching of pigments *in vivo* might also occur in response to impaired PS II; however, it remains possible that photoinhibition at the PS I side occurs simultaneously *in vivo*. Further studies are necessary to fully understand the effects of pigment replacement.

Acknowledgments

This study was supported by a Grant-in-Aid for Creative Scientific Research (17GS0314) to MM and AT from the Japanese Society for the Promotion of Science (JSPS), and by Grants-in-Aid for Scientific Research from the Japanese Ministry of Education, Culture, Sports, Science, and Technology (MEXT) to T Tomo (19614007) and SA (18350067).

References

[1] W.M. Manning, H.H. Strain, Chlorophyll *d*, a green pigment of red algae, J. Biol. Chem. 151 (1943) 1–19.
[2] R. Tanaka, A. Tanaka, Tetrapyrrole biosynthesis in higher plants, Annu. Rev. Plant Biol. 58 (2007) 321–346.
[3] R.J. Porra, Recent progress in porphyrin and chlorophyll biosynthesis, Photochem. Photobiol. 63 (1997) 492–516.
[4] X. Lin, H.A. Murchison, V. Nagarajan, W.W. Parson, J.P. Allen, J.C. Williams, Specific alteration of the oxidation potential of the electron donor in reaction centers from *Rhodobacter sphaeroides*, Proc. Natl. Acad. Sci. U. S. A. 91 (1994) 10265–10269.
[5] K. Artz, J.C. Williams, J.P. Allen, F. Lendzian, J. Rautter, W. Lubitz, Relationship between the oxidation potential and electron spin density of the primary electron donor in reaction centers from *Rhodobacter sphaeroides*, Proc. Natl. Acad. Sci. U. S. A. 94 (1997) 13582–13587.
[6] V.V. Klimov, S.I. Allakhverdiev, S. Demeter, A.A. Krasnovsky, Photoreduction of pheophytin in photosystem 2 of chloroplasts with respect to redox potential of the medium, Dokl. Akad. Nauk SSSR 249 (1979) 227–230.
[7] F. Rappaport, M. Guergova-Kuras, P.J. Nixon, B.A. Diner, J. Lavergne, Kinetics and pathways of charge recombination in photosystem II, Biochemistry 41 (2002) 8518–8527.
[8] G. Renger, Functional pattern of photosystem II, In: G. Renger (Ed.), Primary Processes of Photosynthesis — Part 2, RSC publishing, UK, 2008, pp. 237–292.
[9] J. Fajer, I. Fujita, M.S. Davis, A. Forman, L.K. Hanson, K.M. Smith, Photosynthetic energy transduction: spectral and redox characteristics of chlorophyll radicals *in vitro* and *in vivo*, In: K.M. Kadish (Ed.), Electrochemical and spectrochemical studies of biological redox components, American chemical society, Washington, D. C, 1982, chapter 21.
[10] L.L. Maggiora, J.D. Petke, D. Gopal, R.T. Iwamoto, G.M. Maggiora, Experimental and theoretical studies of Schiff base chlorophylls, Photochem. Photobiol. 42 (1985) 69–75.
[11] M. Kobayashi, S. Ohashi, K. Iwamoto, Y. Shiraiwa, K. Yuki, T. Watanabe, Redox potential of chlorophyll *d in vitro*, Biochim. Biophys. Acta 1767 (2007) 597–602.
[12] S. Satoh, M. Ikeuchi, M. Mimuro, A. Tanaka, Chlorophyll *b* expressed in cyanobacteria functions as a light-harvesting antenna in photosystem I through flexibility of the proteins, J. Biol. Chem. 276 (2001) 4293–4297.
[13] N. Nagata, R. Tanaka, S. Satoh, A. Tanaka, Identification of a vinyl reductase gene for chlorophyll synthesis in *Arabidopsis thaliana* and implications for the evolution of *Prochlorococcus* species, Plant Cell 17 (2005) 233–240.
[14] M. Mimuro, A. Tanaka, The *in vitro* and *in vivo* reconstitution of pigment–protein complexes, and its implication in acquiring a new system, Photosynth. Res. 81 (2004) 129–137.
[15] H. Xu, D. Vavilin, W. Vermaas, Chlorophyll *b* can serve as the major pigment in functional photosystem II complexes of cyanobacteria, Proc. Natl. Acad. Sci. U. S. A. 98 (2001) 14168–14173.
[16] S. Akimoto, M. Yokono, M. Ohmae, I. Yamazaki, N. Nagata, R. Tanaka, A. Tanaka, M. Mimuro, Excitation energy transfer in the antenna system with divinyl-chlorophylls in the vinyl reductase-expressing *Arabidopsis*, Chem. Phys. Lett. 409 (2005) 167–171.
[17] H. Ito, M. Yokono, R. Tanaka, A. Tanaka, Identification of a novel vinyl reductase gene essential for the biosynthesis of monovinyl chlorophyll in *Synechocystis* sp. PCC6803, J. Biol. Chem. 283 (2008) 9002–9011.
[18] M.R. Islam, S. Aikawa, T. Midorikawa, Y. Kashino, K. Satoh, H. Koike, *slr*1923 of *Synechocystis* sp. PCC6803 is essential for conversion of 3,8-divinyl(proto) chlorophyll(ide) to 3-monovinyl(proto)chlorophyll(ide), Plant Physiol. 148 (2008) 1068–1081.
[19] T.M. Bricker, J. Morvant, N. Masri, H.M. Sutton, L.K. Frankel, Isolation of a highly active photosystem II preparation from *Synechocystis* 6803 using a histidine-tagged mutant of CP47, Biochim. Biophys. Acta 1409 (1998) 50–57.

[20] M. Mimuro, S. Akimoto, T. Tomo, M. Yokono, H. Miyashita, T. Tsuchiya, Delayed fluorescence observed in the nanosecond time region at 77 K originates directly from the photosystem II reaction center, Biochim. Biophys. Acta 1767 (2007) 327–334.
[21] R.J. Porra, W.A. Thompson, P.E. Kriedemann, Determination of accurate extinction coefficients and simultaneous equations for assaying chlorophylls *a* and *b* extracted with four different solvents: verification of the concentration of chlorophyll standards by atomic absorption spectroscopy, Biochim. Biophys. Acta 975 (1989) 384–394.
[22] Y. Shimada, T. Tsuchiya, S. Akimoto, T. Tomo, M. Fukuya, K. Tanaka, M. Mimuro, Spectral properties of the CP43-deletion mutant of *Synechocystis* sp. PCC6803, Photosynth. Res. 98 (2008) 303–314.
[23] T. Tomo, T. Okubo, S. Akimoto, H. Miyashita, T. Tsuchiya, T. Noguchi, M. Mimuro, Identification of the special pair of photosystem II in a chlorophyll *d*-dominated cyanobacterium, Proc. Natl. Acad. Sci. U. S. A. 104 (2007) 7283–7288.
[24] T. Tomo, Y. Kato, T. Suzuki, S. Akimoto, T. Okubo, T. Noguchi, K. Hasegawa, T. Tsuchiya, K. Tanaka, M. Fukuya, N. Dohmae, T. Watanabe, M. Mimuro, Characterization of highly purified photosystem I complexes from the chlorophyll *d*-dominated cyanobacterium *Acaryochloris marina* MBIC 11017, J. Biol. Chem. 283 (2008) 18198–18209.
[25] D.V. O'Connor, D. Phillips, Time-Correlated Single Photon Counting, Academic Press, London, 1984, Ch. 2.
[26] M.J. Frisch, G.W. Trucks, H.B. Schlegel, G.E. Scuseria, M.A. Robb, J.R. Cheeseman, J.A. Montgomery Jr., T. Vreven, K.N. Kudin, J.C. Burant, J.M. Millam, S.S. Iyengar, J. Tomasi, V. Barone, B. Mennucci, M. Cossi, G. Scalmani, N. Rega, G.A. Petersson, H. Nakatsuji, M. Hada, M. Ehara, K. Toyota, R. Fukuda, J. Hasegawa, M. Ishida, T. Nakajima, Y. Honda, O. Kitao, H. Nakai, M. Klene, X. Li, J.E. Knox, H.P. Hratchian, J.B. Cross, V. Bakken, C. Adamo, J. Jaramillo, R. Gomperts, R.E. Stratmann, O. Yazyev, A.J. Austin, R. Cammi, C. Pomelli, J.W. Ochterski, P.Y. Ayala, K. Morokuma, G.A. Voth, P. Salvador, J.J. Dannenberg, V.G. Zakrzewski, S. Dapprich, A.D. Daniels, M.C. Strain, O. Farkas, D.K. Malick, A.D. Rabuck, K. Raghavachari, J.B. Foresman, J.V. Ortiz, Q. Cui, A.G. Baboul, S. Clifford, J. Cioslowski, B.B. Stefanov, G. Liu, A. Liashenko, P. Piskorz, I. Komaromi, R.L. Martin, D.J. Fox, T. Keith, M.A. Al-Laham, C.Y. Peng, A. Nanayakkara, M. Challacombe, P.M.W. Gill, B. Johnson, W. Chen, M.W. Wong, C. Gonzalez, J.A. Pople, Gaussian 03 Revision C.02, Gaussian Inc., Wallingford CT, 2004.
[27] H.-C. Chow, R. Serlin, C.E. Strouse, The crystal and molecular structure and absolute configuration of ethyl chlorophyllide *a* dehydrate. A model for the different spectral forms of chlorophyll *a*, J. Am. Chem. Soc. 97 (1975) 7230–7237.
[28] A.D. Becke, A new mixing of Hartree–Fock and local density-functional theories, J. Chem. Phys. 98 (1993) 5648–5652.
[29] C. Lee, W. Yang, R.G. Parr, Development of the Colle–Salvetti correlation-energy formula into a functional of the electron density, Phys. Rev. B 37 (1988) 785–789.
[30] V.P. Shedbalkar, C.A. Rebeiz, Chloroplast biogenesis: determination of the molar extinction coefficients of divinyl chlorophyll *a* and *b* and their pheophytins, Anal. Chem. 207 (1992) 261–266.
[31] M. Alfonso, G. Montoya, R. Cases, R. Rodriguez, R. Picorel, Core antenna complexes, CP43 and CP47, of higher plant photosystem II. Spectral properties, pigment stoichiometry, and amino acid composition, Biochemistry 33 (1994) 10494–10500.
[32] G. Shen, W.F.J. Vermaas, Chlorophyll in a *Synechocystis* sp. PCC6803 mutant without photosystem I and photosystem II core complexes, J. Biol. Chem. 269 (1994) 13904–13910.
[33] A. Telfer, J.D.L. Rivas, J. Barber, β-carotene within the isolated photosystem II reaction center: photooxidation and irreversible bleaching of this chromophore by oxidized P680, Biochim. Biophys. Acta 1060 (1991) 106–114.
[34] T. Tomo, E. Hirano, J. Nagata, K. Nakazato, Pigment exchange of photosystem II reaction center by chlorophyll *d*, Photosynth. Res. 84 (2005) 77–83.
[35] A.H. Salter, I. Virgin, Å. Hagman, B. Andersson, On the molecular mechanism of light-induced D1 protein degradation in photosystem II core particles, Biochemistry 31 (1992) 3990–3998.
[36] R. Barbato, C.A. Shipton, G.M. Giacometti, J. Barber, New evidence suggests that the initial photoinduced cleavage of the D1-protein may not occur near the PEST sequence, FEBS Lett. 290 (1991) 162–166.
[37] E.M. Aro, I. Virgin, B. Andersson, Photoinhibition of photosystem II. Inactivation, protein damage and turn over, Biochim. Biophys. Acta 1143 (1993) 113–134.
[38] M. Mimuro, I. Yamazaki, S. Itoh, N. Tamai, K. Satoh, Dynamic fluorescence properties of D1–D2–cytochrome *b*-559 complex isolated from spinach chloroplasts: analysis by means of the time-resolved fluorescence spectra in picosecond time range, Biochim. Biophys. Acta 933 (1988) 478–486.
[39] Z. Vokáčová, J.V. Burda, Computational study on spectral properties of the selected pigments from various photosystems: structure–transition energy relationship, J. Phys. Chem. A 111 (2007) 5864–5878.
[40] T. Tomo, S. Akimoto, T. Tsuchiya, M. Fukuya, K. Tanaka, M. Mimuro, Isolation and spectral characterizaion of photosystem II reaction center from *Synechocystis* sp. PCC6803, Photosynth. Res. 98 (2008) 293–302.
[41] B. Loll, J. Kern, W. Saenger, A. Zouni, J. Biesiadka, Towards complete cofactor arrangement in the 3.0 Å resolution structure of photosystem II, Nature 438 (2005) 1040–1044.
[42] B. Andersson, J. Barber, Mechanisms of photodamage and protein degradation during photoinhibition of photosystem II, In: N.R. Baker (Ed.), Photosynthesis and the Environment, Kluwer, Dordrecht, The Netherlands, 1996, pp. 101–121.
[43] C. Spetea, T. Hundal, F. Lohmann, B. Andersson, GTP bound to chloroplast thylakoid membranes is required for light-induced, multienzyme degradation of the photosystem II D1 protein, Proc. Natl. Acad. Sci. U. S. A. 96 (1999) 6547–6552.
[44] M. Lindahl, C. Spetea, T. Hundal, A.B. Oppenheim, Z. Adam, The thylakoid FtsH protease plays a role in the light-induced turnover of the photosystem II D1 protein, Plant Cell 12 (2000) 419–431.
[45] N. Mizusawa, T. Tomo, K. Satoh, M. Miyao, Degradation of the D1 proteins of photosystem II under illumination *in vivo*: two different pathways involving cleavage or intermolecular cross-linking, Biochemistry 42 (2003) 10034–10044.
[46] T. Noguchi, T. Tomo, C. Kato, Triplet formation on a monometric chlorophyll in the photosystem II reaction center as studied by time-resolved infrared spectroscopy, Biochemistry 40 (2001) 2176–2185.
[47] E. Schlodder, T. Renger, G. Raszewski, W.J. Coleman, P.J. Nixon, R.O. Cohen, B.A. Diner, Site-directed mutations at D1-thr179 of photosystem II in *Synechocystis* sp. PCC 6803 modify the spectroscopic properties of the accesory chlorophyll in the D1-branch of the reaction center, Biochemistry 47 (2008) 3143–3154.
[48] T.M. Bricker, L.M. Frankel, The structure and function of the 33 kDa extrinsic protein of photosystem II: a critical assessment, Photosynth. Res. 56 (1998) 157–173.
[49] I. Enami, A. Okumura, R. Nagao, T. Suzuki, M. Iwai, J.-R. Shen, Structure and functions of the extrinsic proteins of photosystem II from different species, Photosynth. Res. 98 (2008) 349–363.
[50] G. Rocap, F.W. Larimer, J. Lamerdin, S. Malfatti, P. Chain, N.A. Ahlgren, A. Arellano, M. Coleman, L. Hauser, W.R. Hess, Z.I. Johnson, M. Land, D. Lindell, A.F. Post, W. Regala, M. Shah, S.L. Shaw, C. Steglich, M.B. Sullivan, C.S. Ting, A. Tolonen, E.A. Webb, E.R. Zinser, S.W. Chisholm, Genome divergence in two *Prochlorococcus* ecotypes reflects oceanic niche differentiation, Nature 424 (2003) 1042–1047.